Journal of the Korean Physical Society, Vol. 65, No. 2, July 2014, pp. 176∼184

An Engineering Method to Estimate the Junction Temperatures of Light-Emitting Diodes in Multiple LED Application

Xing Fu, Run Hu and Xiaobing Luo*
School of Energy and Power Engineering, Huazhong University of Science and Technology, Wuhan 430074, China

(Received 14 January 2014)

Acquiring the junction temperature of light emitting diode (LED) is essential for performance evaluation. But it is hard to get in the multipleLED applications. In this paper, an engineering method is presented to estimate the junction temperatures of LEDs in multiple LED applications. This method is mainly based on an analytical model, and it can be easily applied with some simple measurements. Simulations and experiments were conducted to prove the feasibility of the method, and the deviations among the results obtained by the present method with those by simulation as well as experiments are less than 2% and 3%, respectively. In the final part of this study, the engineering method was used to analyze the thermal resistances of a street lamp. The material of leadframe was found to affect the system thermal resistance mostly, and the choice of solder material strongly depended on the material of the leadframe.

PACS numbers: 44.05.+e
Keywords: LED array, Junction temperature, Engineering method, Analytical model, Thermal resistance
DOI: 10.3938/jkps.65.176

I. INTRODUCTION

Light-emitting diodes (LEDs) have been widely used because they have many advantages [1]. For LED applications, the junction temperatures of the LEDs are extremely important, because it affects the reliability and optical performance significantly. Because of the low power of a single LED chip, usually multiple LEDs are used to meet the lumen demand for applications such as LED street lamps, LED vehicle lamps, LED backlight screens and so on. So far, a junction temperature tester can measure the junction temperature of a single LED chip well, but getting the junction temperatures for multiple LEDs is not easy.

Generally, three ways exist to get the junction temperature of an LED, which are by tester measurement, by simulation and by analytical method. Measurement by a tester is a basic way to get the junction temperature. For a single LED die, we can get the junction temperature conveniently by using electrical testing methods [2–4] or optical testing methods [5,6]. However, both the electrical and the optical testing methods can only achieve the mean junction temperature for multiple LEDs. Other measurement methods, for example, using temperature sensors [7], are also difficult to use in multiple LEDs. In addition, the present junction temperature tester is very expensive and is difficult to apply widely in industry and in research institutes.

Compared with direct measuring with equipment, simulation is flexible and convenient, and is widely used to analyze the temperature for both single-LED and multiple-LED applications [8]. However, simulation is only convenient for a professional modeling engineer, but is a hard work for most people. Also, any change in the simulation model, such as the heat transfer rate, thermal conductivity and component dimensions, requires a new simulation. Especially, when the model's dimensions change, new mesh must be divided, which will take much time for the multiple-LED applications because of the large substrate and tiny LED die.

The analytical method, which is advantageous for analyzing the effects of dimensional changes and changing in other variables, is widely used in the microelectronic industry [9,10]. Some works on the thermal analysis of LED applications by many analytical solutions have been conducted by our group [11–13]. However, the previous work mostly focused on part of the structure for LED applications, for example, the system level, and could not be used to obtain the junction temperatures of multiple LEDs.

In this paper, we propose an engineering method based on an analytical solution to predict the junction temperature in multipleLEDs applications with typical structures. In the analytical solution, the typical structure is divided into four parts, and an analytical model is built in series for each part. To validate this engineering method, simulations and experiments were conducted.

*E-mail: luoxb@hust.edu.cn; Fax: +86-27-87540724

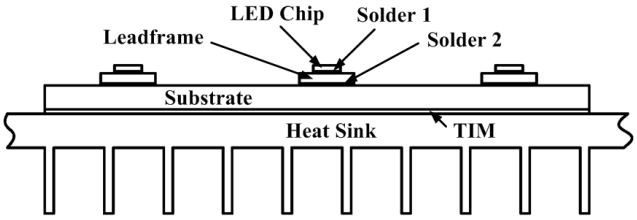

Fig. 1. Typical structure for multiple LED application.

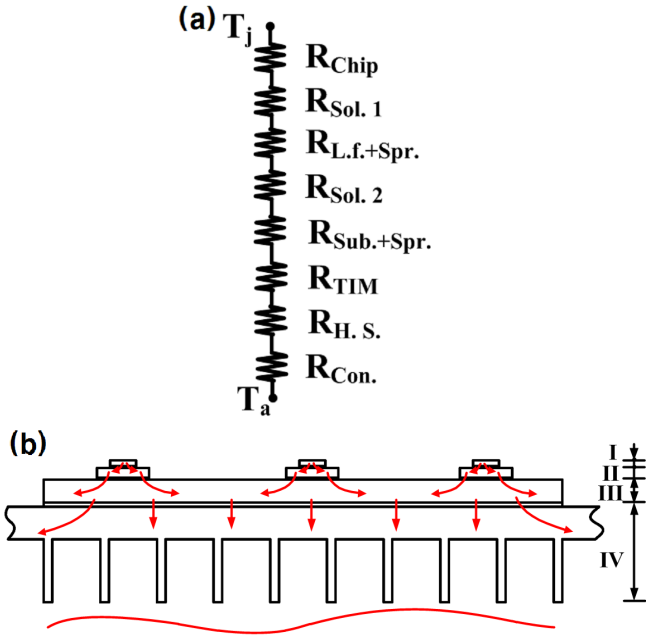

Fig. 2. (Color online) (a) Thermal resistance network and (b) Division of the multiple LEDs structure.

The results show that this method cam be used to predict the junction temperature and can be used for product optimization.

II. MODEL ESTABLISHING

A typical structure for multiple-LED applications is shown in Fig. 1. The LED chip is bonded on a leadframe, which is mainly composed of copper, silicon, or ceramic. The leadframe is then bonded on a substrate, which is connected with heat sink by thermal interface material (TIM). The heat sinks are usually fin radiators because of their good reliability. The structure in Fig. 1 is the most common design for most LED products, but in some other applications, LED chips may be mounted on the substrate directly; all of them will be included in our analytical model and engineering method.

Because of the small area and low temperature, the heat radiated from the chip to the air is very little, and most of the heat generated by the LED chip is conducted

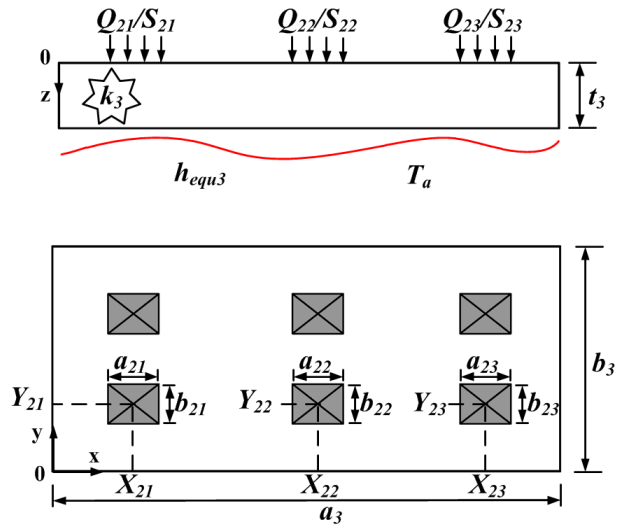

Fig. 3. (Color online) Schematic for part III modeling.

through the leadframe and substrate to the heat sink, and finally dissipated to the air by convection. Because nearly all the heat generated by LEDs is dissipated by the heat sink, the edge and the top surfaces of the leadframe, the substrate, the solders and the TIM can be treated as adiabatic. As conductive areas obviously vary at the interface between the LED chip and the leadframe as well as between the leadframes and the substrate, a spreading thermal resistance occurs. The thermal resistance network of the structure shown in Fig. 1 is indicated in Fig. 2(a). When the multiple-LED structure is treated as a whole, getting an analytical solution is difficult, so we divide the structure into four parts as shown in Fig. 2(b). Part I, part II, part III and part IV contain the LED chip and the solder 1, the leadframe and the solder 2, the substrate, and the TIM and the heat sink, respectively. The thermal resistance and the temperature rise in each part would be calculated as follow: For part II and part III, spreading thermal resistances exist. Many researches have been done about how to deal with them [14–21], and here we will adopt existing methods.

Part III contains the substrate as shown in Fig. 1. The main purpose of this part is to acquire the temperatures of the bottom surfaces of part II, which are treated as heat sources in this part. The schematic for part III is indicated in Fig. 3. The thermal power for the j_{th} heat source is Q_{2j}; the source is located at (X_{2j}, Y_{2j}) with dimensions of $a_{2j} \times b_{2j}$. The thermal conductivity of the substrate is k_3, and its dimension is$a_3 \times b_3 \times t_3$. All the T_a which appears in this paper is ambient temperature. The h_{equ3} is the equivalent convective coefficient of the bottom surface of the substrate, which we will obtain by simple measurement as discussed in a later part of this paper. Here we just treat it as a known number.

As multiple heat sources exist, the temperature of each source is the collective effect of all heat sources. The mean temperature excess of the j_{th} heat source $\overline{\theta_{2j}}$ over

the region $S_{2j} = a_{2j} \times b_{2j}$ can be obtained by the expressions proposed by Muzychka *et al.* [14]:

$$\overline{\theta_{2j}} = \sum_{i=1}^{N} \frac{1}{S_{2j}} \iint_{A_{2j}} \theta_{2i}(x, y, 0)\, dS_{2j} = \sum_{i=1}^{N} \overline{\theta_{2i}}, \tag{1}$$

with

$$\begin{aligned} \overline{\theta_{2i}} &= A_0^i + 2\sum_{m=1}^{\infty} A_m^i \frac{\cos(\lambda_m X_{2j}) \sin(\frac{1}{2}\lambda_m a_{2j})}{\lambda_m a_{2j}} + 2\sum_{n=1}^{\infty} A_n^i \frac{\cos(\delta_n Y_{2j}) \sin(\frac{1}{2}\delta_n b_{2j})}{\delta_n b_{2j}} \\ &+ 4\sum_{m=1}^{\infty}\sum_{n=1}^{\infty} A_{mn}^i \frac{\cos(\delta_n Y_{2j}) \sin(\frac{1}{2}\delta_n b_{2j}) \cos(\lambda_m X_{2j}) \sin(\frac{1}{2}\lambda_m a_{2j})}{\lambda_m a_{2j} \delta_n b_{2j}} \end{aligned} \tag{2}$$

where N is the number of heat sources, and $\overline{\theta_{2i}}$ is the mean temperature excess over the region concerned of $S_{2j} = a_{2j} \times b_{2j}$ located at (X_{2j}, Y_{2j}). A_0^i, A_m^i, A_n^i and A_{mn}^i are the calculated coefficients for the i_{th} source. λ_m, β_n, and δ_{mn} are eigenvalues for the solution. These parameters can be described as follows:

$$\lambda_m = {}^{m\pi}/_{a_3}, \tag{3}$$

$$\delta_n = {}^{n\pi}/_{b_3}, \tag{4}$$

$$\beta_{mn} = \sqrt{\lambda_m^2 + \delta_n^2}, \tag{5}$$

$$A_0^i = \frac{Q_{2i}}{a_3 b_3}\left(\frac{t_3}{k_3} + \frac{1}{h_{equ3}}\right), \tag{6}$$

$$A_m^i = \frac{4Q_{2i} \cos(\lambda_m X_{2i}) \sin(\frac{1}{2}\lambda_m a_{2i})}{a_3 b_3 a_{2i} \lambda_m^2 k_3 \phi(\lambda_m)}, \tag{7}$$

$$A_n^i = \frac{4Q_{2i} \cos(\delta_n Y_{2i}) \sin(\frac{1}{2}\delta_n b_{2i})}{a_3 b_3 b_{2i} \delta_n^2 k_3 \phi(\delta_n)}, \tag{8}$$

$$A_{mn}^i = \frac{16Q_{2i} \cos(\lambda_m X_{2i}) \sin(\frac{1}{2}\lambda_m a_{2i}) \cos(\delta_n Y_{2i}) \sin(\frac{1}{2}\delta_n b_{2i})}{a_3 b_3 a_{2i} b_{2i} k_3 \beta_{mn} \lambda_m \delta_n \phi(\beta_{mn})}, \tag{9}$$

where Q_{2i} is the thermal power generated by the i_{th} heat source, Φ is the spreading function for the Eqs. (7)-(9), and $\Phi(\lambda_m), \Phi(\beta_n)$*, and* $\Phi(\delta_{mn})$can be obtained by replacing the dummy variable ζ with λ_m, δ_n, and β_{mn} in the equation below:

$$\phi(\zeta) = \frac{\zeta \sinh(\zeta t_3) + h_{equ3}/k_3 \cosh(\zeta t_3)}{\zeta \cosh(\zeta t_3) + h_{equ3}/k_3 \sinh(\zeta t_3)} \tag{10}$$

Part II contains the leadframe and solder 2 as shown in Fig. 1. The main purpose of part II is to obtain the temperature of the bottom surface of part I, which is treated as a heat source in this part. The schematic for part II is indicated in Fig. 4. The upper bulk is the leadframe, and the lower bulk is solder 2. As shown in Fig. 4, the thermal power for the j_{th} heat source is Q_{1j}; the source is located at (X_{1j}, Y_{1j}) with dimensions of $a_{1j} \times b_{1j}$. The thermal conductivities and the dimensions of the leadframe and the solder 2 arek_2 and$a_{2j} \times b_{2j} \times t_{2j}$, and$k_{20}$ and$a_{2j} \times b_{2j} \times t_{20j}$, respectively. The h_{equ2j} is the equivalent convective coefficient of the bottom surface of the j_{th}leadframe.

From the analysis of part III, we have already gotten the mean temperature excess of the bottom surface of part II, $\overline{\theta_{2j}}$, so we can get the equivalent convective thermal coefficient h_{equ2} with the equation below:

$$h_{equ2j} = \frac{Q_{1j}}{a_{2j} b_{2j} \overline{\theta_{2j}}}. \tag{11}$$

Different from the structure of part III, here the heat source is a single source, while solder 2 below the leadframe makes it a compound system, which is not thermally isotropic. The mean temperature excess $\overline{\theta_{1j}}$ of the heat source on the j_{th} leadframe over the region of $S_{1j} = a_{1j} \times b_{1j}$ can be obtained by the expressions proposed by Yovanovich *et al.* [15]:

$$\overline{\theta_{1j}} = A_0^j + 2\sum_{m=1}^{\infty} A_m^j \frac{\cos(\lambda_m X_{1j})\sin(\frac{1}{2}\lambda_m a_{1j})}{\lambda_m a_{1j}} + 2\sum_{m=1}^{\infty} A_n^j \frac{\cos(\delta_n Y_{1j})\sin(\frac{1}{2}\delta_n b_{1j})}{\delta_n b_{1j}} + 4\sum_{m=1}^{\infty}\sum_{m=1}^{\infty} A_{mn}^j \frac{\cos(\delta_n Y_{1j})\sin(\frac{1}{2}\delta_n b_{1j})\cos(\lambda_m X_{1j})\sin(\frac{1}{2}\lambda_m a_{1j})}{\lambda_m a_{1j}\delta_n b_{1j}}, \quad (12)$$

where A_0^j, A_m^j, A_n^j and $A_{mn}^j$are the calculated coefficients for the j_{th} source. λ_m, β_n, δ_{mn} are the eigenvalues for the equation. They can be obtained as follows:

$$\lambda_m = m\pi/a_{2j}, \quad (13)$$

$$\delta_n = n\pi/b_{2j}, \quad (14)$$

$$\beta_{mn} = \sqrt{\lambda_m^2 + \delta_n^2}, \quad (15)$$

$$A_0^j = \frac{Q_{1j}}{a_{2j}b_{2j}}\left(\frac{t_{2j}}{k_{2j}} + \frac{t_{20j}}{k_{20j}} + \frac{1}{h_{equ2j}}\right), \quad (16)$$

$$A_m^j = \frac{4Q_{1j}\cos(\lambda_m X_{1j})\sin(\frac{1}{2}\lambda_m a_{1j})}{a_{2j}b_{2j}a_{1j}\lambda_m^2 k_2 \phi(\lambda_m)}, \quad (17)$$

$$A_n^j = \frac{4Q_{1j}\cos(\delta_n Y_{1j})\sin(\frac{1}{2}\delta_n b_{1j})}{a_{2j}b_{2j}b_{1j}\delta_n^2 k_2 \phi(\delta_n)}, \quad (18)$$

$$A_{mn}^j = \frac{16Q_{1j}\cos(\lambda_m X_{1j})\sin(\frac{1}{2}\lambda_m a_{1j})\cos(\delta_n Y_{1j})\sin(\frac{1}{2}\delta_n b_{1j})}{a_{2j}b_{2j}a_{1j}b_{1j}k_2\beta_{mn}\lambda_m\delta_n\phi(\beta_{mn})}, \quad (19)$$

where Φ is the spreading function for Eqs. (17)-(19), and $\Phi(\lambda_m)$, $\Phi(\beta_n)$, $\Phi(\delta_{mn})$ can be obtained by replacing the dummy variable ζ with λ_m, δ_n, β_{mn} in the equation below:

$$\phi(\zeta) = \frac{(\alpha e^{4\zeta t_{2j}} - e^{2\zeta t_{2j}}) + \rho(e^{2\zeta(2t_{2j}+t_{20j})} - \alpha e^{2\zeta(t_{2j}+t_{20j})})}{(\alpha e^{4\zeta t_{2j}} + e^{2\zeta t_{2j}}) + \rho(e^{2\zeta(2t_{2j}+t_{20j})} + \alpha e^{2\zeta(t_{2j}+t_{20j})})}, \quad (20)$$

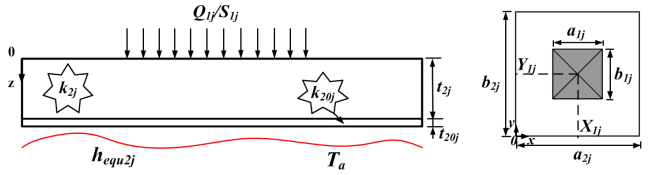

Fig. 4. (Color online) Schematic for part II modeling.

where

$$\alpha = \frac{1 - k_{20j}/k_{2j}}{1 + k_{20j}/k_{2j}}, \quad (21)$$

$$\rho = \frac{\zeta + h_{equ2j}/k_{20j}}{\zeta - h_{equ2j}/k_{20j}}. \quad (22)$$

Part I includes the LED chip and solder 1 as shown in Fig. 1. The purpose of part I is to obtain the junction temperature of the LED chip. The schematic for part I is indicated in Fig. 5. The upper bulk is the LED chip, and the lower bulk is solder 1. The thermal resistance of the LED chip is usually provided by the manufacturer. The thermal conductivities and the dimensions of solder 1 are k_{10} and$a_{1j} \times b_{1j} \times t_{10j}$, respectively. $\overline{T_{1j}}$ is

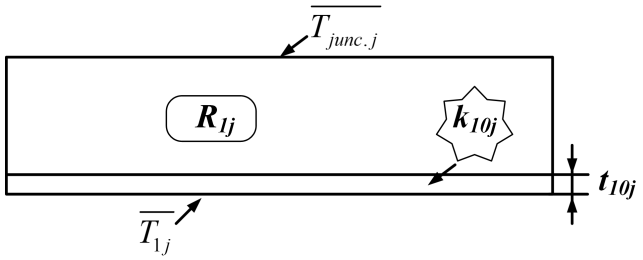

Fig. 5. Schematic for part I modeling.

the mean temperature of the bottom surface of solder 1 counted on the j_{th}leadframe, which can be calculated by the following equation:

$$\overline{T_{1j}} = \overline{\theta_{1j}} + T_a, \quad (23)$$

where $\overline{\theta_{1j}}$ has already been obtained in the analysis of part II.

The junction temperature of the j_{th}LED chip, $\overline{T_{junc,j}}$, can be acquired by the following equations:

$$\overline{T_{junc,j}} = Q_j(R_{1j} + R_{10j}) + \overline{T_{1j}}, \quad (24)$$

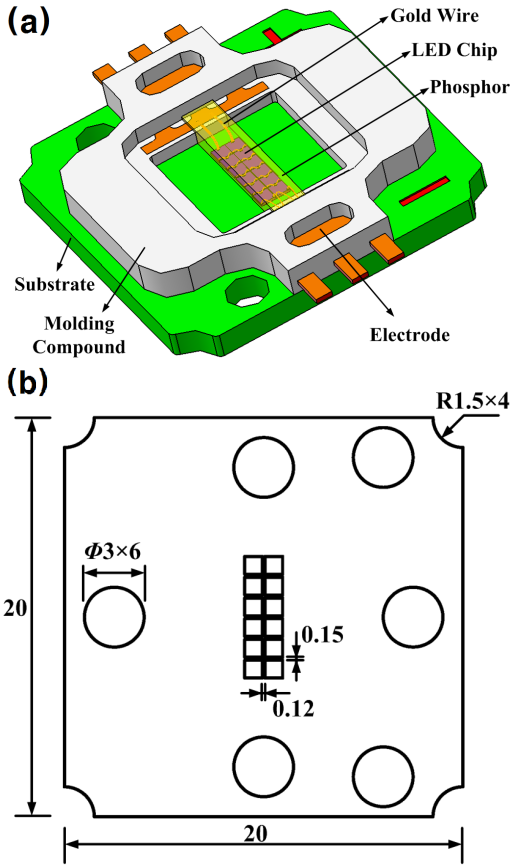

Fig. 6. (Color online) (a) Multiple LED module and (b) Schematic of the module (unit: mm).

where Q_j is the thermal power generated by the j_{th}LED chip. $R_{1j}R_{10j}$ is the thermal resistance between the junction and the bottom of the LED chip, which is usually provided by the manufacturer. R_{10j} is the thermal resistance of solder 1 and is given by

$$R_{10j} = \frac{t_{10j}}{a_{1j}b_{1j}k_{10j}}. \tag{25}$$

The equivalent convective coefficient at the substrate bottom, h_{equ3} was treated as a known parameter in the analysis for part III. Here, we provide a method to get the h_{equ3}. As the TIM is usually grease or some other soft material, mounting thermocouples at the bottom surface of the substrate is feasible, so we can measure the temperatures of the surface directly. Then, the mean temperature of the surface, $\overline{T_{3b}}$, can be obtained, and the h_{equ3} can be calculated with the following equation:

$$h_{equ3} = \sum_{j=1}^{N} Q_j \Big/ a_3 b_3 (\overline{T_{3b}} - T_a). \tag{26}$$

The engineering method based on the analytical model is achieved after completing the above four steps. For the chip on board (CoB) packaging, because its structure

ITO	100nm
p-GaN	150nm
p-$Al_xGa_{1-x}N$	50nm
MQW($In_yGa_{1-y}N$/GaN)	100nm
n-GaN	4μm
Buffer Layer	50nm
Substrate(Sapphire)	100μm
Reflecting Layer(Ag)	100nm
Bonding Layer	

Fig. 7. (Color online) Typical structure of a conventional LED chip.

is simpler and has fewer layers compared with the one shown in Fig. 1, we can use the same method to get the junction temperature.

III. MODEL VALIDATION

For experimental convenience, we chose a compact CoB packaging application to validate the present method, as indicated in Fig. 6, where the LED chips are mounted on a copper substrate directly, so there are no leadframe and solder 2. The LED chip used is the conventional LED, whose typical structure is shown in Fig. 7. A multiple quantum well (MWQ) layer, which is the socalled junction, is seen to be very close to the top surface of the LED chip, and materials between the junction and the top surface are highly conductive, so the thermal resistance between them is very little. Thermocouples were used to measure the temperatures on the bottom surface of the substrate, so the equivalent convective coefficient of the bottom surface can be obtained with the Eq. (26).

We compared the experimental results, simulation results and engineering method results. A thermal infrared imaging (IR) camera was adapted to measure the temperatures of the top surfaces of the LED chips. For accurate measurement, the emissivity of the LED's surface should be obtained. In our experiment, we first measured the junction temperature with a junction tester. Then, the IR imaging camera was used to measure the surface temperature of the LED chip. Because the die size is small, we can use the junction temperature obtained from the junction temperature tester to calibrate

Table 1. Parameters for multiple LEDs.

	Length (mm)	Width (mm)	Thickness (mm)	Bottom Surface Area (mm^2)	Conductivity (W/(mK))
Substrate	20	20	1.5	350.52	400
Solder 1	0.89	0.89	0.015	-	48.12
Chip	0.89	0.89	0.15	-	25.12

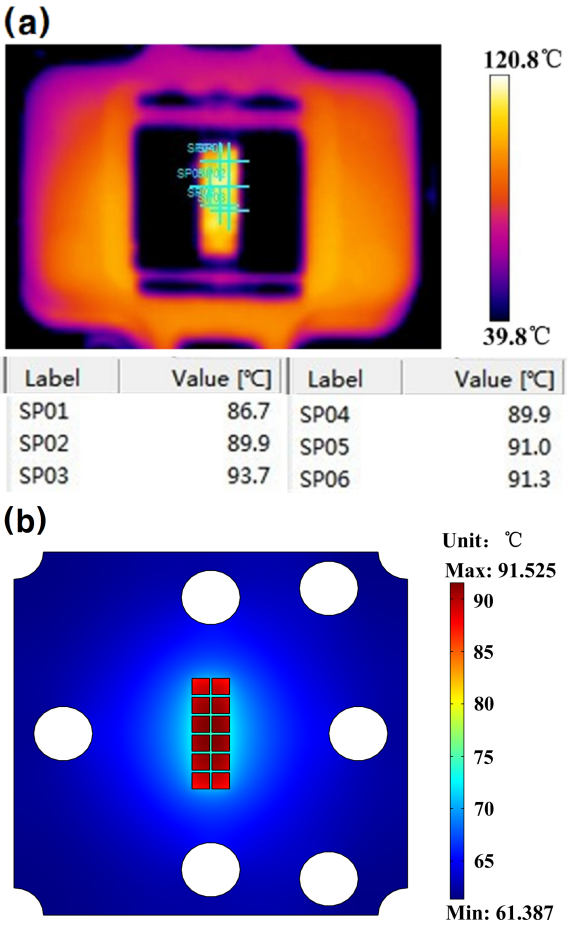

Fig. 8. (Color online) (a) Infrared image (b) Simulation result.

the surface temperature achieved by the IR experiment;, thus we can get the emissivity accurately.

The commercial software COMSOL Multiphysics was used to simulate the temperature field for the module. To simplify the simulation, we ignored the little thermal affected components such as the molding compound, electrode, phosphor, and gold wire that experienced only slight thermal effects. The thermal resistance of the LED chip was obtained from the manufacturer. To get a direct temperature display of the LED chip, we treated it as a uniform bulk with a thermal conductivity, which was calculated by the known thermal resistance of the LED

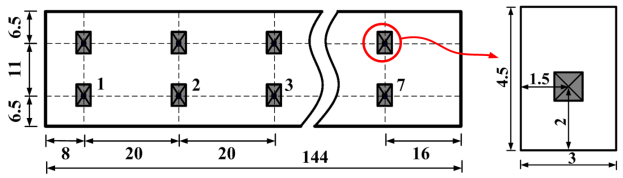

Fig. 9. (Color online) Dimensions of one street lamp.

chip. The top surfaces of LED chips were loaded with the same heatgeneration rate. The bottom surface of the substrate was given an equivalent convective coefficient.

The engineering method was used to estimate the junction temperatures. In this case, the heat generation rate and the dimension of each heat source were the same. The heat generated by each LED chip was 2.087 W, and the other parameters used are listed in Table 1. The substrate in our model was a rectangul, and while the substrate here is not fully regular, we use the equivalent length for the present engineering method.

The infrared image and the simulation result for the multipleLED module are shown in Fig. 8. As the module is horizontally symmetric, we choose six LED chips to compare. The junction temperatures acquired by the engineering method, simulation and measurement are listed in Table 2. From Table 2, we see that the errors between the simulations and the engineering method are less than 2% and that errors between the experiments and the engineering method are less than 4%, which means the present engineering method model is sufficient for engineering use. Therefore, this engineering method based on an analytical model is feasible for use to evaluate the junction temperatures in multiple LED applications.

IV. APPLICATION AND ANALYSIS

We applied the present engineering method to estimate the junction temperatures of a LED street lamp, which has the typical structure shown in Fig. 1. The dimensions and the related parameters are indicated in Fig. 9 and Table 3.Junction temperatures of each LED based on the engineering method and simulations are listed in Table 4. Errors between the engineering method results and simulation results are less than 1%.

Table 2. Comparison of junction temperatures among the engineering method, simulation, and experiment.

	Junction Temperature (°C)					
Engineering method	88.1	89.7	90.4	88.1	89.7	90.4
Simulation	88.6	90.3	91.0	88.7	90.3	91.0
Experiment	86.7	89.9	93.7	89.9	91.0	91.3
	Error					
Simulation vs. Engineering method	1.32%	1.58%	1.58%	1.58%	1.58%	1.58%
Experiment vs. Engineering method	−1.61%	0.22%	3.52%	2.00%	1.43%	0.99%
Experiment vs. Simulation	−2.14%	−0.44%	2.97%	1.35%	0.78%	0.33%

Table 3. Parameters of the LED street lamp.

	Substrate	Solder 2	Leadframe	Solder 1	Chip
Length (mm)	144.00	3.00	3.00	0.89	0.89
Width (mm)	24.00	4.50	4.50	0.89	0.89
Thickness (mm)	2.00	0.03	0.50	0.03	0.15
Conductivity (W/(m·K))	18.50	48.12	41.30	48.12	25.12
Q (W)	1.74	h_{equ3} (W/(m^2·K))	288.7	T_a(°)	18.0

Table 4. Junction temperatures of the LED street lamp.

Chip Number	1	2	3	4	5	6	7
Eng. Method (°C)	95.31	93.65	93.36	93.3	93.21	92.77	90.23
Simulation (°C)	95.98	94.19	93.88	93.81	93.72	93.23	90.48
Error	0.70%	0.57%	0.55%	0.55%	0.54%	0.50%	0.27%

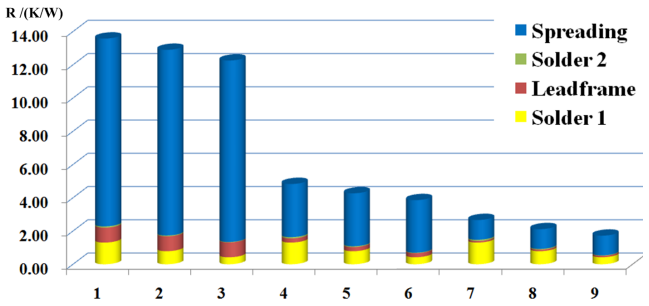

Fig. 10. (Color online) Comparison of thermal resistances for different materials with different components.

For the LED street lamp or other multipleLED applications, it is better to know each part of the thermal resistance and the total system thermal resistance. This will provide guidance to choose the correct materials to decrease the junction temperatures of the LEDs and to save the money. We compared the thermal resistances when different materials were used in LED applications. In this comparison, the materials of solder 1 and solder 2 were the same. The materials are listed in Table 5.The comparison of the thermal resistances for different materials with different components in LED applications is indicated in Fig. 10. The horizontal coordinate means the case number shown in Table 5, and the vertical coordinate means the thermal resistance. The material of the leadframe is found to affect the system thermal resistance mostly. When the material of the leadframe is changed from ceramic to silicon and then copper, the system thermal resistance changes form 13.58 K/W to 4.83 K/W and then 2.66 K/W with solder of Ag grease. The maximum reduction in the system thermal resistance is as high as 80.4%. We also found no need to use expensive solders when the thermal conductivity of the leadframe was low (for example, ceramic). When the material of the leadframe was ceramic, the proportion of

Table 5. Different leadframe and solder materials.

Leadframe Material	Thermal Conductivity W/(m·K)	Solder Material	Thermal Conductivity W/(m·K)	Case Number
Ceramic	41.3	Ag Grease	29.0	1
		Pb-Sn Solder	48.1	2
		Nano-Ag Grease	90.0	3
Silicon	148.0	Ag Grease	29.0	4
		Pb-Sn Solder	48.1	5
		Nano-Ag Grease	90.0	6
Copper	400.0	Ag Grease	29.0	7
		Pb-Sn Solder	48.1	8
		Nano-Ag Grease	90.0	9

thermal resistance of the leadframe to the system thermal resistance was 6.6% when the material of solder 1 was Ag grease. The low proportion means that using better solder is insignificant. We also found that solders with high thermal conductivity were more effective when the thermal conductivity of the leadframe was high (such as silicon and copper). When the material of the leadframe was copper, the proportion of the thermal resistance of solder 1 to the system thermal resistance was as high as 49.1% when solder 1 was Ag grease, which could be reduced to 24.5% when the material of solder 1 was changed to nano-Ag grease. In addition, there was no need to use expensive materials for solder 2. The proportion of the thermal resistance of solder 2 to the system thermal resistance was less than 3% for all situations in this comparison, which means that using a better solder for solder 2 is meaningful.

V. CONCLUSION

An engineering method based on an analytical model to estimate the junction temperatures of LEDs in multiple LED applications was presented in this paper. Simulations and experiments were conducted to validate the method, and comparisons showed that the deviations between results obtained using the present method and that obtained using simulations as well as experiments were less than 2% and 3%, respectively. The engineering method was also used to analyze the thermal resistances of a street lamp, and the material of the leadframe was found to affect the system thermal resistance mostly and to influence the choice of the solder.

ACKNOWLEDGMENTS

The authors would like to acknowledge the financial support in part from the National Natural Science Foundation of China (51376070) and in part from the 973 Project of the Ministry of Science and Technology of China (2011CB013105).

REFERENCES

[1] S. Liu and X. B. Luo, *LED Packaging for Lighting Applications: Design, Manufacturing, and Testing* (John Wiley Press, USA, 2011).
[2] Q. Chen, X. B. Luo, S. J. Zhou and S. Liu, Rev. Sci. Instrum. **82**, 084904 (2011).
[3] A. Keppens, W. R. Ryckaert, G. Deconinck and P. Hanselear, J. Appl. Phys. **104**, 093104 (2008).
[4] Q. Chen, X. B. Luo, R. Chen, S. Wang, Z. H. Chen and S. Liu, *Proc. 2011 International Conference on Electronic Packaging Technology & High Density Packaging*, (Shanghai, China, Aug. 13-16, 2011), p. 924.
[5] Y. Xi, J. Q. Xi, T. Gessmann, J. M. Shah, J. K. Kim, E. F. Schubert, A. J. Fischer, M. H. Crawford, K. H. A. Bogart and A. A. Allerman, Appl. Phys. Lett. **86**, 031907 (2005).
[6] Z. Vaitonis, P. Vitta and A. Zukauskas, J. Appl. Phys. **103**, 093110 (2008).
[7] C. Y. Lee, A. Su, Y. C. Liu and W. Y. Fan, Sensors **9**, 7 (2009).
[8] S. Jang and M. W. Shin, IEEE T. Device Mat. Res. **8**, 3 (2008).
[9] X. B. Luo, Z. M. Mao, J. Liu and S. Liu, Thermochim. Acta **512**, 1 (2011).
[10] A. Bar-Cohen, T. Elperin and R. Eliasi, IEEE Trans. Comp. Hybrids, Manuf. Technol. **12**, 4 (1989).
[11] X. B. Luo, T. Cheng, W. Xiong, Z. Y. Gan and S. Liu, IET Optoelectron. **1**, 5 (2007).
[12] X. B. Luo, W. Xiong and S. Liu, *Proc. 2008 International Conference on Electronic Packaging Technology & High*

Density Packaging, (Shanghai, China, July 28-31, 2008), p. 216.
[13] T. Cheng, X. B. Luo, S. Y. Huang and S. Liu, Int. J. Therm. Sci. **49**, 1 (2010).
[14] Y. S. Muzychka, J. R. Culham and M. M. Yovanovich, J. Electron. Packaging **125**, 2 (2003).
[15] M. M. Yovanovich, Y. S. Muzychka and J. R. Culham, J. Thermophys. Heat Tr. **13**, 4 (1990).
[16] Y. S. Muzychka, M. M. Yovanovich and J. R. Culham, J. Thermophys. Heat Tr. **18**, 1 (2004).
[17] Y. S. Muzychka, M. Stevanovic and M. M. Yovanovich, J. Thermophys. Heat Tr. **15**, 3 (2001).
[18] Y. S. Muzychka, M. M. Yovanovich and J. R. Culham, *Proc. 39th AIAA Aerospace Sciences Meeting & Exhibit*, (Reno, NV, USA, AIAA 01-0366, January 8-11, 2001).
[19] Y. S. Muzychka, M. M. Yovanovich and J. R. Culham, *Proc. 36th AIAA Thermophysics Conference*, (Orlando, Florida, USA, AIAA 2003-4187, June 23-26, 2003).
[20] Y. S. Muzychka, M. M. Yovanovich and J. R. Culham, *Proc. 36th AIAA Thermophysics Conference*, (Orlando, Florida, USA, AIAA 2003-4188, June 23-26, 2003).
[21] X. B. Luo, Z. M. Mao and S. Liu, Int. J. Therm. Sci. **50**, 11 (2011).